# NUMERICAL SIMULATION ON $NO_X$ REDUCTION IN THE FLOAT GLASS FURNACE WITH GRADIENT OXYGEN-ENHANCED COMBUSTION

***Mingfang Jin*** [*1], ***Feng He*** [2], ***Junlin Xie*** [2], ***Shuxia Mei*** [1]

[*1]Department of Material Science and Engineering, Wuhan University of Technology, Wuhan, China

[2]Faculty of Materials and Manufacturing, Beijing University of Technology, Beijing 100124, China

[*] Corresponding author; E-mail: 111jmf@163.com

Abstract: *To reveal the influence of using gradient oxygen-enhanced combustion on the gas flow, combustion status, heat transfer and nitrogen oxide (NOx) emission in glass furnace, numerical simulation on the flame space of an actual float glass furnace with air combustion was conducted. The streamline of combustion-supporting gas and flue gas was displayed, the temperature distribution and heat transfer performance in the flame space were analyzed, and the mechanism of NOx emission reduction by gradient oxygen-enhanced combustion was explored. The comparative study between air combustion and gradient oxygen-enhanced combustion showed that there is not much difference in the streamline and temperature distribution in flame space, which ensures the stability of working state in furnace. Compared with air combustion, the temperature of the batch zone was increased by using gradient oxygen-enhanced combustion, and the high-temperature combustion zone was closer to the glass surface, which increases the radiant heat flux to the glass surface. In addition, the NOx emission concentration in flue gas at the outlets was reduced by 17.1%. The results obtained in this study not only provide important theoretical guidance for gradient oxygen-enhanced combustion in glass furnace, but also lay a foundation for further research about advanced combustion mode to save energy and reduce emissions.*

**Key words: float glass furnace; flame space; gradient oxygen-enhanced combustion; numerical simulation; NOx emission reduction**

## 1. Introduction

With the awareness of public to protect environment increasing, the energy saving and emission reduction technology of the glass industry continues to develop[1,2]. The oxygen-enhanced combustion is a NOx emission reduction technology that using pure oxygen burning in local region of glass furnace based on the traditional air combustion technology. The key to this technology is to reduce part of the combustion-supporting air and supplement with rich oxygen or pure oxygen[3]. J. Pedel found that a small amount of oxygen injected near the outlet of ports can burn out the remaining CO and reduce NOx[4]. However, it has not been used to inject pure oxygen at the inlet of ports in float glass furnace. With gradient oxygen-enhanced combustion technology, the gas composition in the combustion space changes, so that the glass furnace also needs to be structured accordingly. Huang Zhibin[5,6] made corresponding improvement guidance on the structure of the regenerator, melting region and cooling region after using the oxygen-enhanced combustion technology in float glass furnace. However, the application of this technology in large float glass furnaces lacks theoretical guidance, and its heat transfer theory and NOx emission reduction mechanism require further research. The glass furnace likes a complex high-temperature reactor, and the traditional cold model experiment can't catch the chemical reaction characteristics, radiative heat transfer process and NOx formation theory of fuel combustion. CFD numerical simulation technology has become an indispensable technical means to solve such problems.

Based on the principles of fluid mechanics and heat transfer, the CFD numerical simulation technology of glass furnace uses computer software to predict the process of gas flow, heat transfer and chemical reactions in glass furnaces by solving mathematical models, etc[7]. In 1990s, Thomas K[8] modeled a low NOx emission systems and provided a good start for the numerical simulation of industrial NOx emission reduction. In 2009, Boineau[9] studied the flameless oxidation technology for NOx emission reduction in glass furnace. In 2010, Manoj K.Choudhary[10] did some research on describing the phenomena of the gas flow and heat transfer in the glass production process with mathematical models. In 2010, Karimi Hamzeh Jafar[11] calculated radiation heat flux, energy consumption, thermal efficiency of furnace, and modeled using the FVM considering the effects of furnace walls and billets. Compared with the reference furnace (oxygen content in air is 21%), the variation trend of NOx emission under different oxygen enrichment levels was studied. It was found that the optimum oxygen content is between 21% and 45% (volume fraction), and the energy consumption per ton of steel can be reduced by increasing oxygen concentration. In 2015, Mette Bugge[12] predicted the fuel combustion process and revealed the chemical kinetic mechanism of NOx formation by using numerical simulation.In 2017,in order to investigate the liquid fuel combustion in gas turbine engine, By comparing the numerical simulation results with the experimental data, Hou Xingxia[13] found and verified the feasibility of the Realizable k-epsilon turbulence model, the non-premixed combustion model and the DO heat transfer model in the strong swirl combustion chamber. In 2019,Dekterev AA[14] numerically simulated the jet and process of diesel fuel combustion of an original evaporation-type burner. A mathematical model was established to investigate the influence of various turbulence models, combustion simulation methods and response schemes. In 2021, Fordoei E Ebrahimi[15] investigated the different characteristics of MILD oxygen-enriched and oxy-methane combustion such as heat transfer, ignition delay, flame color, flame structure, emissions of CO and NOx (as air pollutants) by the adding of $CO_2$ to the oxidizer with CFD simulation. The results indicated that MILD oxygen-enriched and oxy-methane combustion have distinct advantages than MILD methane-air combustion involving enhancing the temperature uniformity about 10-15%, more distributed reaction zone and a significant reduction of NOx emission. In order to investigate the effect of gradient oxygen-enhanced combustion on status and nitrogen oxide reduction in glass furnace, in this paper, a model of a float glass furnace burning heavy oil is established firstly, then the combustion, heat transfer and nitrogen oxide formation in the flame space with air combustion and gradient oxygen-enhanced combustion are simulated respectively. By comparing and analyzing the simulation results, the effects and principles of NOx reduction of gradient oxygen-enhanced combustion will be explored. The research results will provide important theoretical reference for the application of gradient oxygen-enhanced combustion technology to reduce NOx emission in the actual glass furnace.

## 2. Models and Numerical Solution Method

### 2.1. Geometrical Model

The object of this paper is the combustion space of a float glass furnace with a capacity of 600 tons per day. Fig. 1 presents the structure diagram of melting region, the model and the mesh of the combustion space. Its dimensions are 39.6 m long, 12.3 m wide, and with arc-shaped crown. Fig. 1(a) shows that there are seven pairs of ports, while the ports on one side are air inlets, the other side of ports are outlets of flue gas. The inlet and outlet are exchanged every 20 minutes because of the symmetrical structure of the float glass furnace. The spacing of each pair of port is 3.3 meters. The ports of No.1 to No.6 have the same width with 2 meters, but the width of No.7 port is 1.2 meters. In addition, Fig. 1(b) displays that three burners are installed under each port except the No.7 port with two burners. In the case of air combustion, the preheated high temperature air entered from the ports in one side of the glass furnace reacts completely with the fuel ejected from burners. Meanwhile the flue gas is discharged from the opposite ports.In the case of gradient oxygen-enhanced combustion,oxygen jets were located in the middle of the burners below each port, and their installation position is lower than that of burners. Therefore, there are two oxygen jets under each port of No.1 to No.6,with one oxygen jet under the port of No.7. The shape of all oxygen jets are round with inner diameter of 15 millimeters. In this case,the combustion supporting gas consists of two parts: the air entering from the ports and the oxygen entering from the oxygen jets. For the oxygen-enhanced combustion, the combustion-supporting air entered from each port is reduced. And the amount of oxygen contained in the reduced air is replaced by the oxygen injected from the oxygen jets corresponding to the port. In this way, the oxygen supplied by each port can be kept the same when the two combustion-supporting methods are adopted. The diagram of the two different combustion-supporting methods is shown in Fig. 2.

Fig. 1 (c) shows the model of combustion space of glass furnace for numerical simulation. Fig. 1 (d) shows the mesh of combustion space of glass furnace. The mesh has been repeatedly modified and tried, because the oxygen nozzles are small diameter circular holes, which are connected with the surrounding area when drawing the grid. Therefore, considering the grid quality, calculation accuracy, calculation time cost and other factors, the number of grids is adjusted many times, and the simulation results are compared with the actual data collected to verify. The mesh determined for simulaion was three-dimensional high-quality structured hexahedral mesh, and the mesh distortion ratio is less than 0.3. In order to improve the quality of the mesh and the calculation accuracy of the simulation, the mesh was refined locally at the combustion regions and oxygen inlets.The number of grids is about 5 million. Fig. 1 (e) shows the approximate location of the temperature measurement points on the crown.

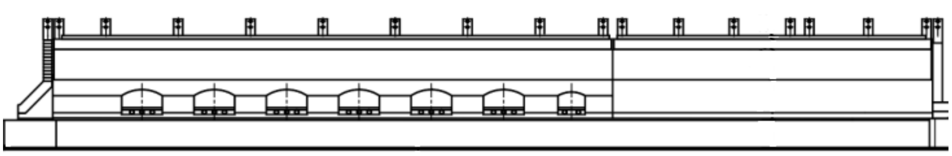

(a) Structure diagram of melting region

(b) Section of port

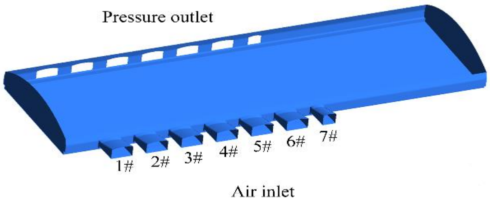


(c) Model of combustion space

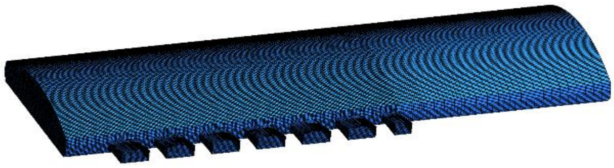

(d) Mesh of combustion space

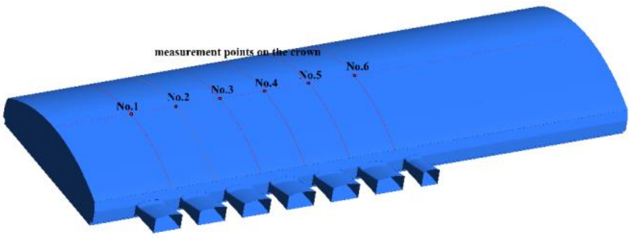


（e）Diagram of temperature measurement points on the crown

**Figure 1** Structure diagram of melting region and mesh of combustion space in glass furnace


(a)Air combustion (b) Gradient oxygen-enhanced combustion

**Figure 2** Diagram of two combustion-supporting technologies.

## 2.2. Mathematical model and Numerical Solution Method

A numerical simulation was conducted using ANSYS Fluent, a popular computational fluid dynamics software. There are gas phase turbulent flow, gas-liquid two-phase flow, fuel burning and radiation heat transfer in the combustion space of the float glass furnace. The following mathematical models are used for the physical and chemical processes.The Realizable k-ε model is used for reflecting turbulent flow, which has shown substantial improvements over the standard k-ε model.[16,17] The realizable k-ε model is suitable for the turbulence-flow features of the glass furnace discussed in this paper.[13] To account for the wall effect in the nearby regions, the wall function was applied to link velocities in the near-wall region. The discrete phase model (DPM) is adopted for gas-liquid two-phase flow to display the atomization process of heavy oil, track the trajectory of droplets and simulate the flow of oil droplets under gravity and resistance conditions.[14] The non-premixed combustion model is selected for indicating chemical reaction of combustion based on diffusion combustion mode actually. The eddy dissipation model (EDM) is chosen for describing interaction between turbulence and chemical reaction.[15] The discrete ordinates (DO) radiation model is used for revealing radiation heat transfer in combustion space, and the weighted-sum-of-gray-gases model (WSGGM) is adopted for reflecting gas radiation characteristics and gas scattering is neglected.[13,17-22] NOx is a pollutant produced in glass furnace. The NOx model in ANSYS FLUENT is used to predict NOx production and analyze the control measures to reduce NOx emission.[15,16]

In solution, the velocity and pressure were coupled using the semi-implicit method for pressure-linked equations (SIMPLE) algorithm in all. For choosing discretization method, STANDARD discrete scheme is selected for the pressure term. The first-order upwind scheme for turbulent energy and radiation is determined by the combination of residuals and convergence,, the second-order upwind scheme is chosen for the others.[17-23] There are no universal metrics for judging convergence. For most problems, the default convergence criterion in ANSYS FLUENT is sufficient. Refers to several similar calculation cases in fluent help, the convergence criterion for energy and radiation terms are less than $1\times10^{-6}$, other items are less than $1\times10^{-3}$.

### 2.3. Boundary Conditions

The setting of boundary conditions in this study is based on actual working conditions. The daily consumption of heavy oil in the glass furnace is 128 t, and the elemental analysis of heavy oil is shown in Tab. 1. Whether air combustion or gradient oxygen-enhanced combustion, the amount of fuel consumption is the same, meanwhile, the fuel distribution ratio and the corresponding excess air coefficient remains unchanged. The percentage of fuel distributed to each port and the corresponding excess air ratio are shown in Tab. 2. The data was obtained according to collection of actual operating parameters of glass furnace. For the oxygen-enhanced combustion, the combustion-supporting air entered from each port is reduced by 8%. And the amount of oxygen contained in the reduced air is replaced by the oxygen injected from the oxygen jets corresponding to the port. In this way, the oxygen supplied by each port can be kept the same when the above-mentioned two combustion-supporting methods are adopted.The purity of oxygen injected from the oxygen jets is 90%.

**Table 1 Element analysis and calorific value of heavy oil**

| **Element** | $C_{daf}$ | $H_{daf}$ | $O_{daf}$ | $N_{daf}$ |
|---|---|---|---|---|
| Mass fraction/% | 83.4 | 12.8 | 3.2 | 0.6 |
| $Q_{net,daf}$/MJ $kg^{-1}$ | | 35.7 | | |

**Table 2 Fuel fraction and excess air factor**

| **Port** | **1#** | **2#** | **3#** | **4#** | **5#** | **6#** | **7#** |
|---|---|---|---|---|---|---|---|
| Fuel fraction /% | 14 | 14 | 15.5 | 15.5 | 18 | 16 | 7 |
| Excess air factor | 1.05 | 1.05 | 1.1 | 1.1 | 1.1 | 1.08 | 1.1 |

The fuel quantity of each burner can be calculated according to the total amount of fuel, burners of each port and the distribution ratio shown in Tab. 2. Heavy oil was preheated to 380 K and atomized into droplets from an atomizer air-blast atomization model, in addition, the droplets were accelerated and injected into furnace. The droplet diameters were distributed according to the Rosin-

Rammler distribution function. The input data was obtained by site collection and reasonable simplification. The combustion air was preheated to 1573 K and the temperature of oxygen is 298 K. The air inlets, oxygen inlets and fuel inlets are set as velocity inlet boundary. Velocity values can be obtained by heat engineering calculation, which require a combination of the inlet area ,gas temperature and excess air ratio of each port in Tab. 2. All outlets are set to pressure outlets of 0.5 Pa. The side wall and the crown are set to convective heat transfer boundary which is one type of the wall boundary, and the heat transfer coefficients are respectively 16.53 $W/m^2·℃$ and 20.34 $W/m^2·℃$ which are obtained by consulting relevant books and based on wall materials and temperature.The temperature distribution at the bottom of combustion space is regular and different in different regions, so the bottom wall was set to temperature boundary and different temperature values were set in different regions. The temperature distribution at the bottom of combustion space can be acquired by polynomial fitting of data collected on site. The function relationship between the bottom temperature of combustion space and the length of furnace is introduced into UDF of FLUENT.

## 3. Results and discussion

### 3.1. Results verification

In order to ensure the validity of the numerical simulation results, the temperature values of the six measurement points on the crown were monitored and compared with the air combustion simulation calculation results, as shown in Tab. 3. The simulated temperature values are in good agreement with that of measured. The maximum difference is 7 ℃. The temperature values of the six measurement points shown in Fig.1(e) are measured by thermocouples commonly used in industry. The difference between the simulated and measured values is within the measurement uncertainty of the thermocouple. Tab. 4 shows the simulated and measured values of the oxygen, nitrogen, carbon monoxide and nitrogen oxides concentrations at the outlets with the air combustion. It can be found that the simulation results are in good agreement with the actual measured data, A comparison of the predicted value and the measured value shows that the simulations are reliable and the method is reasonable.

**Table 3 Temperature values of the measurement points on the crown**

| **Measuring point** | **No.1** | **No.2** | **No.3** | **No.4** | **No.5** | **No.6** |
|---|---|---|---|---|---|---|
| Measured value/K | 1715 | 1765 | 1833 | 1815 | 1795 | 1777 |
| Simulated value/K | 1713 | 1772 | 1835 | 1817 | 1792 | 1774 |

**Table 4 Simulated and measured values of oxygen, nitrogen, carbon monoxide and nitrogen oxides concentrations at each outlet**

| Port number | No.1 | No.2 | No.3 | No.4 | No.5 | No.6 | No.7 |
|---|---|---|---|---|---|---|---|
| Simulated value of oxygen concentration(%) | 2.3 | 2.4 | 5.3 | 2.0 | 3.6 | 1.6 | 6.1 |
| Measured value of oxygen concentration(%) | 2.2 | 2.5 | 5.2 | 2.1 | 3.8 | 1.9 | 5.8 |
| Simulated value of nitrogen concentration(%) | 69.3 | 68.9 | 70.6 | 71.8 | 72.5 | 71.4 | 71.1 |

| | | | | | | | |
|---|---|---|---|---|---|---|---|
| Measured value of nitrogen concentration(%) | 69.6 | 68.5 | 70.9 | 72.1 | 72.4 | 71.2 | 71.3 |
| Simulated value of carbon monoxide concentration(%) | 0.12 | 0.15 | 0.18 | 0.21 | 0.25 | 0.38 | 0.16 |
| Measured value of carbon monoxide concentration(%) | 0.13 | 0.12 | 0.16 | 0.21 | 0.26 | 0.36 | 0.18 |
| Simulated value of nitrogen oxides concentration($mg/m^3$) | 1099 | 1102 | 1033 | 1143 | 1106 | 1235 | 748 |
| Measured value of nitrogen oxides concentration($mg/m^3$) | 1086 | 1079 | 1016 | 1202 | 1121 | 1254 | 806 |

### 3.2. Gas flow

The gas flow characteristics in the flame space has an important influence on the temperature system, pressure stability and heat transfer of the glass furnace. Fig. 3 and Fig. 4 show the gas flow streamlines of glass furnace and No.4 port using air combustion and gradient oxygen-enhanced combustion respectively. Fig. 3 and Fig. 4 showed that large-scale transverse backflow was formed on the right side of the No.7 port, whether air combustion or gradient oxygen-enhanced combustion. The high temperature gas generated by combustion reaction has a long trajectory in the large scale circulation zone of the refining zone, which prolongs the heat exchange time between the high temperature gas at the back of the furnace and the molten glass at the bottom of the combustion space, which is beneficial to the refining of glass.

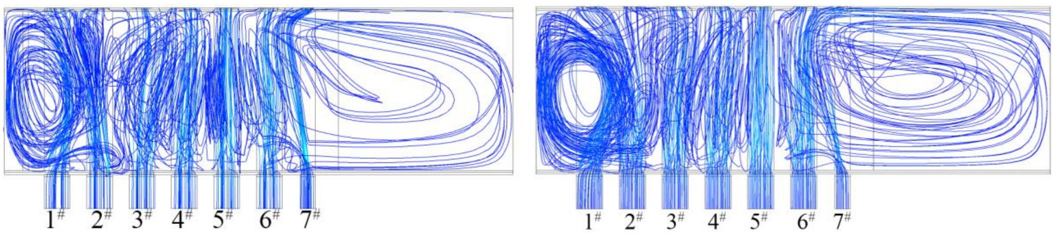


(a) Air combustion (b) Gradient oxygen-enhanced combustion

**Figure. 3** Gas flow streamline of glass furnace

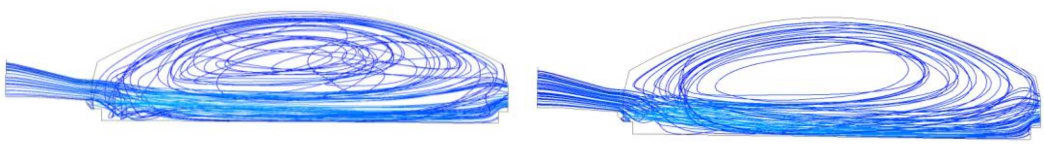

(a) Air combustion (b) Gradient oxygen-enhanced combustion

**Figure 4** Gas flow streamline of No.4 port

Vertically, combustion-supporting gas reacts with fuel after entering the glass furnace. The mixed gas flow flows smoothly from the inlets to the opposite outlets. Most of the gas flow flows out from the outlets, part to upward and forming longitudinal backflow under the crown, and a small part flowing transverse and disturbed with the high temperature gas flow generated by combustion in the adjacent ports.The smooth gas flow closed to the molten glass surface can reduce the erosion and fluctuation of the glass level surface. The longitudinal backflow and transverse backflow makes high-temperature gas quickly fill the combustion space. The backflow formed on the left of the No.1 port can accelerate the melting rate of the batch well, and the backflow area on the right of the No.7 port is large, which is conducive to the uniform heating of the molten glass. So the gas flow characteristics in the glass furnace match the actual production needs, which indicates the rationality of the simulation results.

As seen from Fig. 3 and Fig. 4, during the gradient oxygen-enhanced combustion, the backflow area on the left of No.1 port is bigger, which makes the backflow of No.1 port closer to No.2 port. And, the gas flow streamline near the molten glass surface is denser and smoother.

### 3.3. Temperature system and heat transfer

The reasonable temperature system of combustion space in glass furnace plays an important role in glass preparation. Fig. 5 shows the temperature contours of the combustion central surface. Fig. 6 shows average temperature along the length direction of glass furnace. Fig. 7 shows average temperature along the width direction of No.1 port.

As seen from Fig. 5 and Fig. 6, the combustion characteristics of each port are similar under the two working conditions, indicating that the temperature system is stabilized, in which the maximum temperature of the combustion center is about 2500~2600 K, and the high-temperature flue gas formed by combustion spreads outward from the combustion central area, extending to the outlets of the opposite ports. The temperature of flue gas at outlet is about 1900~2000 K. There are six peak values of temperature peaks located in the combustion center of No.1 to No.6 ports respectively, and the temperature peak values of No.5 port are highest. The temperature peaks in No.7 port is not obvious because the its fuel fraction was relatively least and the combustion zone was close to No.6 port because of the backflow in the back of glass furnace. Overall, the average temperature increases, then decreases rapidly and decreases slowly in the refining zone.

By contrast, the temperature distribution from port No.3 to 7 has little difference under the two working conditions. However, the average temperature under the gradient oxygen-enhanced combustion condition is relatively a little higher. it can be found that the obvious differences of temperature distribution between the two conditions lie in the batch melting zone which is in front of No.2 port, especially at No.1port. Under the gradient oxygen-enhanced combustion working condition, the high-temperature area in the batch zone is larger. In particular, the temperature in the front area of No.1 port is obviously increased, but the maximum temperature decrease at No.2 port because of the larger scale backflow in the front of the glass furnace. The backflow caused the high temperature gas from No.1 port was brought to the front of the glass furnace, so that the residence time of high temperature gas in the furnace is prolonged and the heat transfer efficiency is improved. The average temperature of No.1 port along the width direction becomes more uniform under the gradient oxygen-enhanced combustion working condition(refer to Fig. 7), because the high speed injection of oxygen make the flame become more rigid and the greater entrainment of the backflow, which ensured the temperature at the root of the flame, the temperature of the middle part is increased, and the temperature of the flue gas at the outlet is reduced, so the loss of heat is reduced.

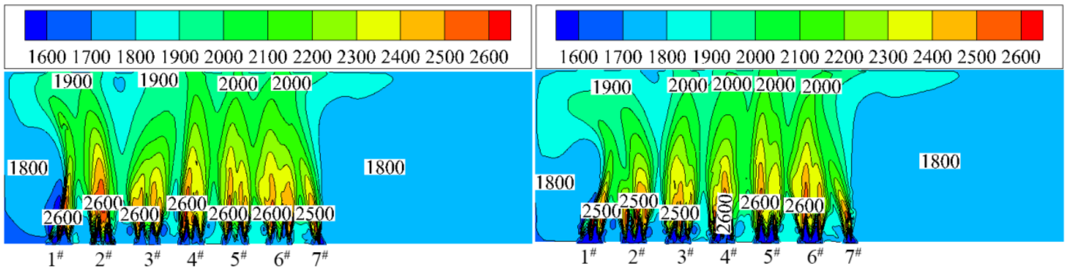


(a) Air combustion (b) Gradient oxygen-enhanced combustion

**Figure 5** Temperature contours of the combustion central surface (K)

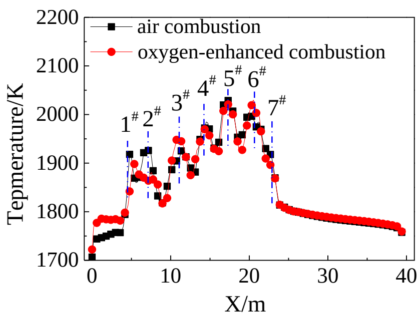


**Figure 6** Average temperature along the length of glass furnace

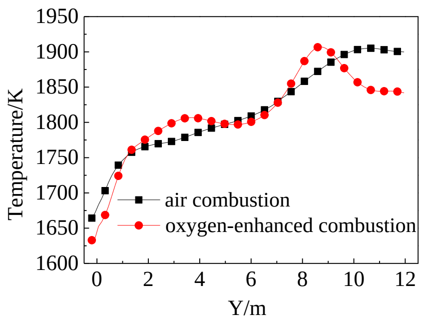


**Figure 7** Average temperature along the width direction of No.1 port

Fig. 8 shows the temperature contours at the vertical slices of No.4 port under the two working conditions.The average temperature curves along the width and height directions of No.4 port under the two working conditions are compared, as shown in Fig. 9. No.4 Port is located in the middle of all the ports, so it is affected by backflow in left and right least and burns stably.Through comparing and analyzing the difference of combustion between the two working conditions, the combustion status and mechanism of the gradient oxygen-enhanced combustion are revealed.

From Fig. 8, in both operating conditions, because the combustion-supporting air enters into the ports sloping downward, the high-temperature zone tends to be close to the molten glass surface, which makes the combustion flame better radiate heat to the molten glass surface. Comparing with air combustion, using gradient oxygen-enhanced combustion technology, the ignition time of fuel is shorter and the initial high temperature area is closer to the molten glass surface. As seen from Fig. 9 (a), along the width direction, before the position about 2 m, the temperature in both working conditions rises rapidly and the temperature values are little different; at the position about 2 ~ 6 m, the average temperature is lower; while at the position after about 6m, the average temperature is higher during air combustion condition. This indicates that using gradient oxygen-enhanced combustion, the reaction speed is faster due to the local $O_2$ concentration increased, and the temperature distribution along the width is more uniform.

As seen from Fig. 9 (b), along the height direction, the trends of temperature are the same under the two working conditions. The temperature rises rapidly to the peak and then decreases rapidly, at last it gradually decreases above about 1.5 m. By comparison, the position of temperature peak is lower and the value of temperature peak is higher during gradient oxygen-enhanced combustion condition. It further illustrates that the combustion is closer to the glass surface and more intense,which is beneficial to the heat transfer of glass surface.

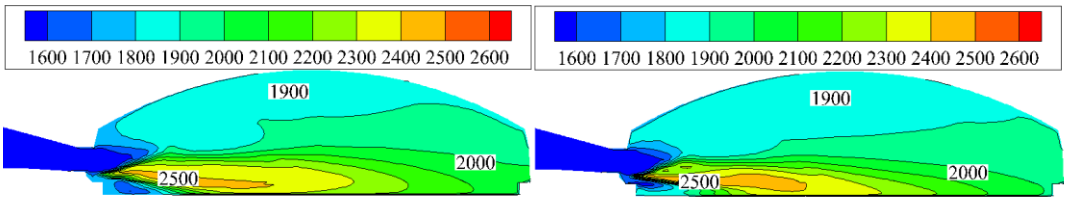


(a) Air combustion (b) Gradient oxygen-enhanced combustion

**Figure 8** Temperature contours at the vertical slices of No.4 port (K)

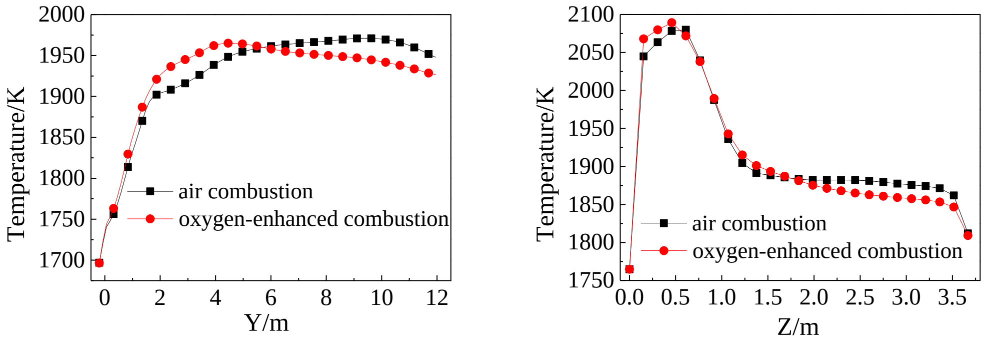


(a) Along the width direction (b) Along the height direction

**Figure 9** Average temperature of No.4 port

Glass preparation requires a lot of heat for melting and silicate reaction. How to transfer heat to molten glass more efficiently is very important for energy saving of glass furnace. Fig. 10 shows the heat flux to the bottom and the total heat flux of the glass furnace. From Fig. 10, compared with the air combustion condition, the total heat flux and the heat flux to the bottom increase by 1.3% and 1.6% respectively under the gradient oxygen-enhanced combustion condition, indicating that the gradient oxygen-enhanced combustion can make better use of the heat of fuel combustion to save energy.

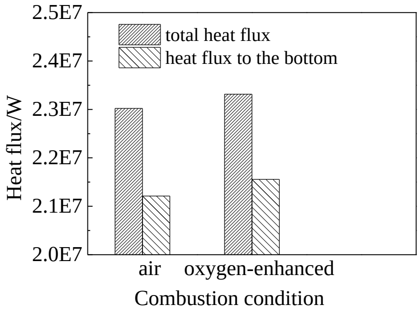


**Figure 10** Heat flux bar chart

### 3.4. NOx emission

NOx is one of the important pollutants in flat glass furnace. It has important industrial and social significance to reduce NOx emissions through improved combustion mode. Tab. 5 shows the NOx concentration at the outlet of each port. As Tab. 5 shows, using gradient oxygen-enhanced combustion, the NOx concentration at the outlets decreased except No.7 outlet, and the average concentration of NOx emission decreases by 17.1%. In fact, the reduction of NOx production is greater, because there is less flue gas due to the reduction of combustion-supporting gas during gradient oxygen-enhanced combustion. Combined with analysis of flow field, the cause for the NOx concentration increasing at the No.7 outlet during gradient oxygen-enhanced combustion is that large scale backflow at the back of the flame space brings flue gas from No.6 port to No.7 outlet, which can be confirmed by the data that the NOx concentration in No.6 outlet is greatly reduced.

**Table 5 NOx concentration at the outlet of each port**

| | **Air combustion /mg•m$^{-3}$** | Gradient oxygen-enhanced combustion /mg•m$^{-3}$ |
|---|---|---|
| No.1 | 1099 | 1024 |
| No.2 | 1102 | 920 |
| No.3 | 1033 | 894 |
| No.4 | 1143 | 802 |
| No.5 | 1106 | 851 |
| No.6 | 1235 | 847 |
| No.7 | 748 | 1003 |
| Average/mg•m$^{-3}$ | 1086 | 900 |
| NOx reduction ratio/% | — | 17.1 |

Fig. 11 shows the average concentration of NOx along the length direction of the glass furnace under the two working condition. As seen from the curves，the trends of the average concentration of NOx in the length direction of the furnace under the two working conditions are similar. But the average concentration values of NOx under the oxygen-enhanced combustion condition are lower than those of the air combustion condition. Under the air combustion working condition, the average concentrations of NOx in the batch melting zone are highest, because there is a large amount of flue gas backflow containing NOx in this area. Then, along the length direction of the furnace, the average concentration of NOx decreases rapidly, and there is a slight change in the centralized combustion area of each port, but there is no obvious peak at No.1 to No.4 ports. The peaks appear at No.5 and No.6 ports and the concentrations reach their maximum, related to the highest temperature in this area. Finally, the average concentrations of NOx decreases rapidly and remain stable in the refining zone. Similarly, the average concentration of NOx is also the highest in the batch melting area under the oxygen-enhanced combustion condition, but the value is much lower than that of the air combustion condition. Along the length direction, the average concentration of NOx decreases slowly. No obvious concentration peak appear at No.1 to No.4 ports. The concentration peaks at port No.5 and No.6 are obvious, but the average concentrations of NOx are lower than those of the batch melting area. In the refining area, NOx concentrations gradually rise, which is caused by flue gas backflow.

In order to reveal a cause of the great decreasing of the average NOx concentration during the oxygen-enhanced combustion condition, Fig. 12 and Fig. 13 respectively show the average concentration of NOx and the average mass fraction of $O_2$、CO、$CO_2$ and $N_2$ along the width direction of port No.4 under the two working conditions.

As seen from Fig. 12, under the two working conditions, with the increasing of temperature, NOx concentration rapidly increases to a certain value and remains stable, and the value of the air combustion condition is greater than that of the gradient oxygen-enhanced combustion condition. It is faster to reach the stable value of NOx concentration under the gradient oxygen-enhanced combustion condition. Combined with the analysis of temperature distribution along the width of furnace(Fig. 9(a)), in the case of gradient oxygen-enhanced combustion, the temperature in the flame space along the width increases more rapidly and keeps uniform, which indicates that the formation of nitrogen oxides is related to not only the temperature peak but also the size of high temperature zone. suppresses the formation of nitrogen oxides to a certain extent.

Comparing Fig. 13(a) and (b), it can be seen that the trends of the concentration of each component under the two working conditions are consistent, but the values of a certain component under different working conditions are different, which indicates that the chemical reaction process is different under the two working conditions. In the float glass combustion space, the main reaction during fuel combustion are: $C+O_2 \rightarrow 1/2CO$ and $CO+1/2O_2 \rightarrow CO_2$; the reaction of NOx formation are $N2+O_2 \rightarrow 2NO$ and $2NO+O_2 \rightarrow 2NO_2$. When the fuel enters the combustion space at first, the fuel is rich, so the combustion occurs quickly, and the CO and $CO_2$ are formed at the same time. With the gradual decreasing of fuel, the formation of CO decreases rapidly and the CO formed is further oxidized to $CO_2$. Thus, the amount of $CO_2$ continues to rise slowly and then keeps stable or decreases. In contrast, the peak of mass fraction of CO is lower during the gradient oxygen-enhanced combustion, while peak of the mass fraction of $CO_2$ is relatively higher. Because the mass fraction of $O_2$ near the port is higher, and the combustion reaction of the fuel is more rapid, intense and complete, so more $CO_2$ is produced and less CO is formed.

The emission of nitrogen oxides is mainly thermal NOx and reactions involved fuel NOx and prompt NOx are negligible concerning NOx formation in glass furnace. The extended Zeldovich mechanism is apparently an effective instrument to describe the thermal NOx formation.It reveals that the formation of thermal NOx is related to the region temperature and the concentration of $N_2$ and $O_2$. The formation of NOx increased exponentially with the increase of temperature, positively correlated with the square square root of oxygen concentration, and linearly correlated with nitrogen concentration. The amount of NOx depends on the formation of NOx and the reduction of NOx. With the combustion reaction going on, the temperature rises rapidly, and the reaction of NOx generation occurs. From Fig. 9(a), it can be found that the temperature distribution is more uniform during the gradient oxygen-enhanced combustion, although the temperature reaches a little higher temperature at an early stage in small area located 3 meters away from the port under the oxygen-enhanced combustion condition. But the concentration of $N_2$ in all area is lower than that of air combustion (refer to Fig. 13) because of part of air is replaced by oxygen, and the concentration of $O_2$ kept almost no rise (refer to Fig. 13) because of total amount of $O_2$ under the gradient oxygen-enhanced combustion condition remains the same. So the formation of NOx can be suppressed by gradient oxygen-enhanced combustion to a certain extent. In addition, from Fig. 9(a), iIt can be found that the space with optimal conditions for the formation of NOx are found about 3 meters away from the port under the gradient oxygen-enhanced combustion condition. However, in this case, the location of the highest CO concentration is the same. So the nitrogen oxides formed in the fore part have good reduction conditions, and the amount of nitrogen oxides is less under the gradient oxygen-enhanced combustion condition. Compared with air combustion, the concentration of $N_2$ and the temperature are lower and the concentration of CO is higher in the rear, so the amount of nitrogen oxides did not continue to increase at an early stage under the gradient oxygen-enhanced combustion condition. In a word, the control method of NOx emission reduction by gradient oxygen-enhanced combustion is to reduce the area of local high temperature zone and control the concentration distribution of $O_2$, $N_2$ and CO.

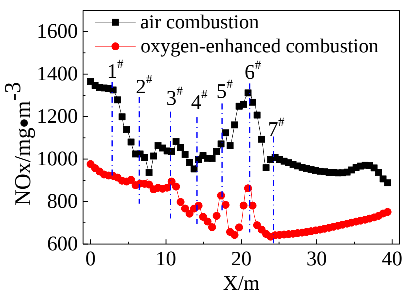


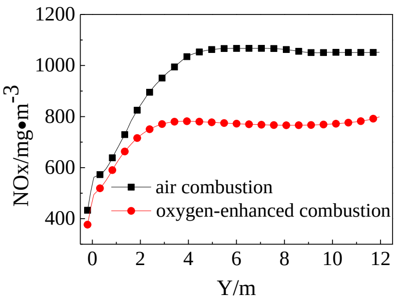


**Figure 11** The average concentration of NOx along the length direction

**Figure 12** The average concentration of NOx along the width direction of No.4 port

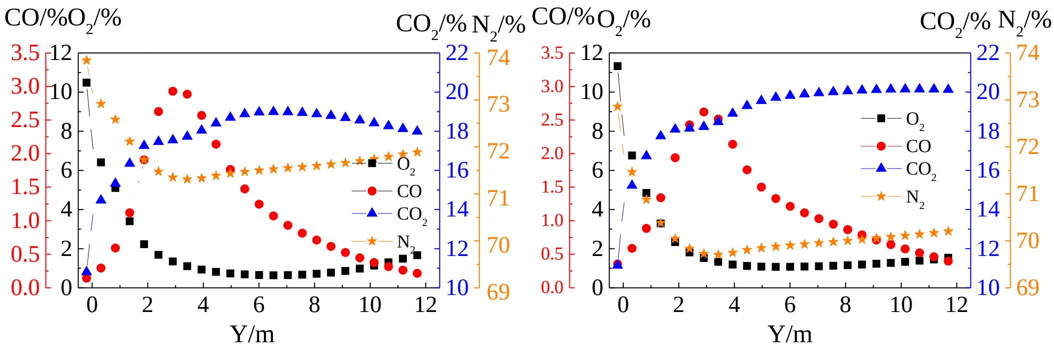


(a) Air combustion (b) Gradient oxygen-enhanced combustion.

**Figure 13** The average mass fraction of $O_2$、CO、$CO_2$ and $N_2$ along the width direction of No.4 port

## 4. Conclusion

Numerical simulation of the flame space of a float glass furnace was carried out, with the simulation results being in good agreement with the actual production data, revealing the simulation results' credibility. The main results were as following:

(1) Whether air combustion or gradient oxygen-enhanced combustion, large-scale transverse circumfluence is formed in the clarification zone in the back of the furnace and obvious circumfluence zone also exists in the front of the furnace. Using gradient oxygen-enhanced combustion, there is larger backflow above the batch, which affects the combustion of fuel at No.1 and No.2 ports.

(2) Under the gradient oxygen-enhanced combustion condition, the combustion in the furnace is more intense and closer to the molten glass, the temperature above the batch is relatively higher, and the temperature distribution along the width is more uniform. The heat transfer efficiency is also better than that of the air combustion.

(3) Compared with the air combustion, the average NOx emission of all ports is reduced by 17.1% with the gradient oxygen-enhanced combustion.

Future work will be focused on the improvement of low NOx combustion technology and engineering application.

## Acknowledgment

This research was funded by the National Key Research and Development Program of China (Grant No.2017YFC0210802).

**References**


[1] Wang Jihua, Application and Comparison of SCR, SNCR and SNCR/SCR Flue Gas Denitration Technology, *Electric Power Technology and Environmental Protection*, 34 (2018), 5, pp. 35-36

[2] Beerkens, Ruud, et al., Reduction of NOx Emissions in Regenerative Fossil Fuel Fired Glass Furnaces: a Review of Literature and Experimental Studies, *Glass Technology*, 49 (2008), 6, pp. 279-288

[3] Zhao Enlu, Zhang wenling, et al., A Section Gradient Oxygen-increasing Combustion Assistance Technology Of Float Glass Furnace for Reducing Emission of NOx, *Glass*, (2013), 5, pp. 12-15

[4] J. Pedel, H. Kobayashi, et al., Oxygen Enhanced NOx Reduction (OENR) Technology for Glass Furnaces, A Collection of Papers Presented at the 75th Conference on Glass Problems, 75th Conference on Glass Problem, Greater Columbus Convention Center, Columbus, Ohio, 2014, pp. 3-6

[5] Huang Zhibin, MU Zhusheng, The Improve Design for Glass Furnace Melter End and Working End of Gradient Increase Combustion Oxygen, *Glass*, (2019), 4, pp. 21-26

[6] Huang Zhibin, MU Zhusheng, The Improve Design for Glass Furnace Regenerator of Gradient Increase Combustion Oxygen, *Glass*, (2018), 9, pp. 17-21

[7] W. Alan Pools, Mathematical Modeling of Glass Melting Systems, *Am Ceram Soc Bul*, 83 (2004), 1, pp. 25-27

[8] Thomas K Dankert, Geoffrey B.Tuson, Demonstration on an Ultra-Low-$NO_x$ Oxygen-fuel Glass Melting System, *Ceram Eng Sci Proc*, 17 (1996), 2, pp. 47-54

[9] Boineau P, Reynes P, et al., Numerical Simulation of a Batch Metallurgy Furnace Equipped with Flameless Oxidation Regenerative Burners, *Revue De Metallurgie*. 104 (2007), 3, pp. 142-148

[10] Manoj K.Choudhary, Raj Venuturumill, et al., Mathematical Modeling of Flow and Heat Transfer Phenomena in Glass Melting, Delivery, and Forming Processes, *International Journal of Applied Glass Science*, 1 (2010), 2, pp. 45-48

[11] Karimi Hamzeh Jafar, Saidi Mohammad Hassan, Heat Transfer and Energy Analysis of a Pusher Type Reheating Furnace Using Oxygen Enhanced Air for Combustion, *IRON AND STEEL RESEARCH INTERNATIONAL*, 17 (2010), 4, pp. 12-17

[12] Mette Bugge, Øyvind Skreiberg, et al., Numerical Simulations of Staged Biomass Grate Fired Combustion with an Emphasis on NOx Emissions, *Energy Procedia*, 75 (2015), pp. 156-161

[13] Hou Xingxia, Wang Shaolin et al., CFD Simulation of Combustion in Gas Turbine Engine, The 5th International Conference on Frontiers of Manufacturing Science and Measuring Technology, 2017, Vol. 6, pp.890-896

[14] Dekterev AA, Minakov AV, et al., Numerical Simulation of Liquid Hydrocarbon Fuel Burning in a Direct-flow Evaporation Burner in a Jet of Superheated Steam, 35th Siberian Thermophysical

Seminar (STS), 2019, pp. 8

[15] Fordoei E. Ebrahimi, Mazaheri Kiumars, et al., Numerical Study on the Heat Transfer Characteristics, Flame Structure, and Pollutants Emission in the MILD Methane-air, Oxygen-enriched and Oxy-methane Combustion, *ENERGY*, (2021), pp. 218

[16] Shuxia Mei, Junlin Xie, et al., Numerical simulation of the complex thermal processes in a vortexing Precalciner, *Applied Thermal Engineering*, 125 (2017), pp. 652–661

[17] Mei Z, Li P, et al., Influences of reactant injection velocities on moderate or intense low-oxygen dilution coal combustion, *Energy & Fuels*, 28 (2014), 1, pp. 369-384

[18] Weber R, Smart J P, et al., On the (MILD) combustion of gaseous， liquid， and solid fuels in high temperature preheated air, *Proceedings of the Combustion Institute*, 30 (2005), 2, pp. 2623-2629

[19] Oscar Díaz-Ibarra, Abad P, et al., Design of a day tank glass furnace using a transient model and steady-state computation fluid dynamics, *Applied Thermal Engineering*, 52 (2013), 2, pp. 555–565

[20] Szymczyk Jacek, Cieslak Ilona, et al., Improvement of Energy Efficiency of Natural Gas Combustion by Applying a Homogeneous Combustion, *E3S Web of Conferences*. 17(2017), pp. 93-96

[21] Banerjee A, Rai A, et al., Simulation of Combustion Space Heat Transfer of Glass Melting Furnace, *Heat Transfer-Asian Research*, (2016)

[22] Abbassi A, Khoshmanesh K, Numerical simulation and experimental analysis of an industrial glass melting furnace, *Applied Thermal Engineering*, *28*(2008), (5-6), pp. 450-459

[23] Miroslav Simcik, Marek C Ruzicka, CFD model for pneumatic mixing with bubble chains: Application to glass melts, *Chemical Engineering Science*, 127(2017), pp. 344-361

Submitted: 01.10.2024
Revised: 21.11.2024
Accepted: 30.11.2024